

The Microwave Anisotropy Probe Attitude Control System

F. L. Markley, S. F. Andrews, J. R. O'Donnell, Jr., D. K. Ward, A. J. Ericsson
NASA's Goddard Space Flight Center, Greenbelt, MD, 20771, USA

Abstract

The Microwave Anisotropy Probe mission is designed to produce a map of the cosmic microwave background radiation over the entire celestial sphere by executing a fast spin and a slow precession of its spin axis about the Sun line to obtain a highly interconnected set of measurements. The spacecraft attitude is sensed and controlled using two inertial reference units, two star trackers, a digital sun sensor, twelve coarse sun sensors, three reaction wheel assemblies, and a propulsion system. This paper describes the design of the attitude control system to carry out this mission and presents some early flight experience.

Introduction

The Microwave Anisotropy Probe (MAP), the second Medium-Class Explorer (MIDEX) mission, was launched on June 30, 2001 as a follow-on to the Cosmic Background Explorer (COBE) satellite, which made unprecedented measurements of the Cosmic Microwave Background (CMB) that is believed to be a remnant of the Big Bang marking the birth of the universe.¹⁻⁴ MAP has been designed to measure the anisotropy in the temperature of the CMB with sensitivity 50 times that of the Differential Microwave Radiometer (DMR) instrument on COBE and angular resolution 30 times finer, specifically 20 microKelvin and 0.23°, respectively.⁵ These increases in sensitivity and resolution will enable scientists to determine the values of key cosmological parameters and to answer questions about the formation of structure in the early universe and the fate of the universe⁶

Since the major error sources in the DMR data arose from COBE's low Earth orbit, MAP was placed in a Lissajous orbit around the Sun-Earth L_2 Lagrange point to minimise magnetic, thermal, and radiation disturbances from the Earth and Sun. MAP attained its Lissajous orbit around L_2 in early October 2001, about 100 days after launch, using a lunar gravity assist following three phasing loops.⁷

The MAP instrument includes radiometers at five frequencies, passively cooled to about 90°K, covering two fields of view (FOVs) 141° apart on the celestial sphere. The MAP observatory executes a fast spin at 0.464 rpm and a slower precession of its spin axis at one revolution per hour at a constant angle of 22.5° from the Sun line to obtain a highly interconnected set of measurements over an annulus between 87° and 132° from the Sun. Figure 1 shows the scan pattern covered by one of the two FOVs in one complete spacecraft precession (1 hour), displayed in ecliptic coordinates in which the ecliptic equator runs horizontally across the map. The bold circle shows the path for a single spin (2.2 minutes). As the Earth revolves around

the Sun, this annulus of coverage revolves about the ecliptic pole. Thus the entire celestial sphere will be observed once every six months, or four times in the planned mission life of two years. This paper will give an overview of the Attitude Control System (ACS) that acquires and maintains the spacecraft orbit, controls the spacecraft angular momentum, provides for safety in the event of an anomaly, and implements the spin-scan observing strategy while minimising thermal and magnetic fluctuations, especially those synchronous with the spin period.

ACS Overview

MAP uses three right-handed, orthonormal co-ordinate systems. The Geocentric Inertial frame (GCI) is an Earth-centred frame with its x_I axis pointing to the vernal equinox, its z_I axis pointing to the North Celestial Pole (parallel to the Earth's spin axis), and $y_I = z_I \times x_I$. The Rotating Sun Referenced frame (RSR) is a spacecraft-centred frame in which the z_R axis points from the MAP spacecraft to the Sun, x_R is a unit vector in the direction of $z_R \times z_I$, and $y_R = z_R \times x_R$. The RSR frame rotates at approximately $1^\circ/\text{day}$ with respect to the GCI frame. The body frame is centred at the spacecraft centre of mass with z_B axis parallel to the spacecraft centreline, directed from the instrument to the solar arrays, y_B axis normal to the instrument radiator faces, and $x_B = y_B \times z_B$, as shown in Figure 2.

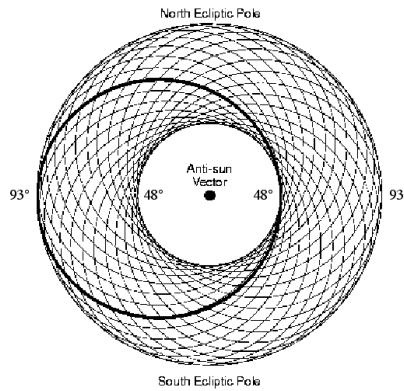


Figure 1: MAP Scan Pattern

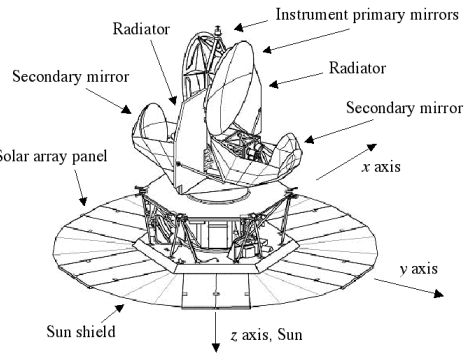


Figure 2: MAP Spacecraft Layout

The attitude sensors employed by the MAP ACS are two two-axis Inertial Rate Units (IRUs), two Autonomous Star Trackers (ASTs), a Digital Sun Sensor (DSS), and twelve Coarse Sun Sensors (CSSs). The spacecraft attitude is controlled by three Reaction Wheel Assemblies (RWAs) and a propulsion system. The RWA rotation axes are tilted 60° from the $-z_B$ axis and uniformly distributed 120° apart in azimuth about this axis. The wheels serve the dual function of counterbalancing the body's spin angular momentum to maintain the system momentum (i.e. body plus wheels) near zero while simultaneously applying torques to control the spacecraft attitude. The wheel axis orientations result in all wheel speeds being biased away from zero during the spin-scan, thus avoiding zero-speed crossings that would occur if the wheel axes were oriented along the spacecraft body frame co-ordinate axes.

The L₂ orbit precludes the use of magnetic sensing or torquing, so the propulsion system is used to unload accumulated system angular momentum after each orbit manoeuvre, several times in the phasing loops but interrupting science observations no more than once every three months at L₂. Gravity-gradient, atmospheric drag, and outgassing torques are significant in the phasing loops; but the accumulated angular momentum of less than 1 Nms per orbit is easily managed. Solar radiation pressure torque is the only significant disturbance torque at L₂, and the uniform rotation of the spin axis reduces its average by more than two orders of magnitude compared to its instantaneous value. Pre-flight estimates of angular momentum accumulation from solar radiation pressure ranged from 0.0016 to 0.065 Nms per day, depending on the accuracy of deployment of the solar arrays and the resulting symmetry of the spacecraft.⁸ The worst-case estimate would reach the Observing Mode system angular momentum limit of 2 Nms, the maximum that can be cycled among the three RWAs at the fast spin rate without adversely affecting attitude control, in 31 days. This would require momentum unloading more frequently than desired; but flight data indicates an angular momentum accumulation of about 0.006 Nms per day, which easily meets the three-month requirement.

ACS Operational Modes

MAP has six ACS modes. Observing, Inertial, Sun Acquisition, Delta V, and Delta H Modes reside in the main spacecraft (Mongoose) processor, while Safehold Mode is implemented in the Attitude Control Electronics (ACE). Anomalies can result in autonomous transitions from any other mode to Safehold or Sun Acquisition Mode.

Observing Mode

Observing Mode is used for science operations to maintain the 22.5°±0.25° angle between the spin axis and Sun line and to implement the observing strategy shown in Figure 1. This is accomplished by specifying the attitude of the MAP spacecraft with respect to the RSR co-ordinate frame by the set of 3-1-3 Euler angles^{9, 10}

$$\phi_c = \phi_0 + \int_{t_0}^t \dot{\phi}_c dt, \quad \theta_c = 22.5^\circ, \quad \text{and} \quad \psi_c = \psi_0 + \int_{t_0}^t \dot{\psi}_c dt, \quad (1)$$

where $\dot{\phi}_c = -1$ rev/hour and $\dot{\psi}_c = 0.464$ rpm are the desired spin-scan rates, and ϕ_0 and ψ_0 are set by the initial state. A commanded RSR-to-body quaternion q_c and a commanded RSR-to-body angular rate vector ω_c are computed from these Euler angles and rates by the standard equations.^{9, 10} The attitude error is expressed as two times the vector part \mathbf{q}_e of an error quaternion q_e , which is the quotient of an estimated RSR-to-body quaternion \hat{q}_{BR} and the commanded quaternion:

$$q_e = \pm \hat{q}_{BR} \otimes q_c^{-1}, \quad (2)$$

with the sign chosen so that the scalar component of q_e is positive. The factor of two reflects the fact that the quaternion error is half the angle error when these are small. In this and the following we use the quaternion product convention of References 10 and 11 rather than that of Reference 9, so that the order of quaternion multiplication is the same as that of the corresponding direction cosine matrices.

The estimated RSR-to-body quaternion \hat{q}_{BR} is computed as

$$\hat{q}_{BR} = \hat{q}_{BI} \otimes q_{RI}^{-1}, \quad (3)$$

where the GCI-to-RSR quaternion q_{RI} is computed onboard from ephemeris models and the estimated GCI-to-body quaternion \hat{q}_{BI} is computed by an onboard Extended Kalman Filter (EKF) with IRU, AST, and DSS measurements as input.^{11, 12} This filter is similar to EKFs employed on several previous missions, except that the AST produces an estimated attitude quaternion rather than merely observed star vectors, removing the burden on the Mongoose processor of star identification and the necessity to carry an onboard star catalogue. A rate error vector $\boldsymbol{\omega}_e$ is given by

$$\boldsymbol{\omega}_e = \hat{\boldsymbol{\omega}}_{BI} - \boldsymbol{\omega}_c, \quad (4)$$

where $\hat{\boldsymbol{\omega}}_{BI}$ is the body rate measured by the IRU, corrected for gyro drifts that are also estimated by the EKF.

The RWA torques are computed by a proportional-derivative (PD) controller in terms of the attitude and rate errors.¹³ Since the commanded attitude is not constant, hangoff error is reduced by adding feedforward to the PD control rather than using integral feedback. The feedforward term includes both the angular acceleration required to follow the commanded attitude and the gyroscopic term needed to move the system momentum \mathbf{H}_{sys} in the body frame as required by its constancy in inertial space. Since $\dot{\phi}_c$, $\dot{\psi}_c$, and $\dot{\theta}_c$ are all constant, the commanded acceleration is:

$$\dot{\boldsymbol{\omega}}_c = \dot{\psi}_c \dot{\phi}_c \sin \theta_c \begin{bmatrix} \cos \psi_c & -\sin \psi_c & 0 \end{bmatrix}^T. \quad (5)$$

The acceleration and gyroscopic terms are added to the commanded PD acceleration to give the total control torque:

$$\mathbf{T} = J \left[k_d \boldsymbol{\omega}_e + k_p (2\mathbf{q}_e) + \dot{\boldsymbol{\omega}}_c \right] + \boldsymbol{\omega}_c \times \mathbf{H}_{sys}, \quad (6)$$

where J is the MAP moment-of-inertia tensor and k_d and k_p are derivative and proportional gains. This torque is distributed to the RWAs using a distribution matrix defined by the orientation of the RWAs in the body co-ordinate system.

Inertial Mode

Inertial Mode acts as a staging mode between the other operations of the spacecraft. This is an RWA- and IRU-based mode similar to Observing Mode, using the same Kalman Filter, but differs in that the commanded rates are zero and the feedforward terms are absent. Inertial Mode can either hold the spacecraft in an inertially fixed orientation or slew the spacecraft to a time-tagged sequence of GCI-to-body quaternions in a Command Quaternion Table (CQT) uploaded from the ground.

Delta V Mode

Delta V Mode is entered from Inertial Mode by ground command to adjust the orbit in the phasing loops and for L₂ stationkeeping. The burn start time and duration, desired attitude (as a single quaternion or a CQT), and direction of the thrust are specified in the command or by table load. Spacecraft attitude is controlled by off-pulsing the thrusters used for the Delta V and on-pulsing the others using IRU and RWA tachometer signals in a PD controller with pulse width modulation.

Delta H Mode

Delta H Mode uses the propulsion system to unload spacecraft system angular momentum, computed using the IRU and RWA tachometers. It is used primarily upon exit from Delta V Mode. The same pulse width modulator is used as for Delta V Mode, but all thrusters are operated in an on-pulsing manner for Delta H Mode.

Sun Acquisition Mode

Sun Acquisition Mode uses the CSS, IRU, and RWAs to acquire and maintain a thermally safe power-positive orientation, with the spacecraft z_B axis within 25° of the Sun. Upon separation from the launch vehicle, Sun Acquisition Mode must slew MAP from any initial angle and any initial body momentum less than [13, 13, 55] Nms to a power-positive orientation within 40 minutes. If the body momentum exceeds the amount that can be handled by Sun Acquisition Mode, the propulsion-based Delta H Mode is entered by ground command to reduce the momentum to an acceptable level, after which the spacecraft returns to Sun Acquisition Mode.

Safehold Modes

The Safehold Mode implemented in the ACE can be entered in the event of a Mongoose anomaly. It has two configurations, which differ by the rate signal used. The first, called Safehold IRU, is a copy of the Sun Acquisition Mode in the Mongoose. The second is a minimum-hardware Safehold Mode using only the RWAs and CSSs, with rate errors being computed by numerically differentiating the position error signals. Since the CSSs are insensitive to rotations about the Sun line, anti-runaway compensation is applied to prevent the wheels from uncontrolled spinning about the satellite's z -axis. This is accomplished by applying equal damping torques to the three wheels if the sum of their speeds exceeds a pre-set value, thereby suppressing z -axis rotation without applying a net torque in the x - y plane. Exit from either Safehold Mode is by ground command only.

Flight Experience

The launch vehicle placed the spacecraft on a very accurate trajectory with body angular momentum of only 6.2 Nms at separation, well within the capability of Sun Acquisition Mode, which acquired the Sun within 15 minutes. Maximum pointing errors during the nine Delta V manoeuvres performed in the first three months of the mission were smaller than predicted (3.7° vs. 5.5°), and imparted velocity increments were accurate to 1%. Less than 15 kg of hydrazine propulsion fuel was expended to get to L_2 , about half the amount budgeted for this phase of the mission. The 57 kg of fuel remaining will easily support a four-year extended mission.

Initially, the precession rate $\dot{\phi}$ in Observing Mode did not meet its 5% accuracy requirement, showing a 7% variation at the spin period. This was attributed to an inaccurate value of system momentum in the gyroscopic feedforward loop arising from a scale factor error in the RWA tachometer signals. Evidence for this was that the magnitude of the system momentum, which should be constant, had a 0.4 Nms oscillation at spin period and increased during spin-up by 1.0 Nms. A high-fidelity

simulation determined that the oscillation and spin-up offset could be removed by a change in the tachometer scale factors of about 2.5% for RWA1 and 4% for RWA2 and RWA3. After loading these new scale factors, the variation of the precession rate was dramatically reduced, as were the spin-period oscillation and the spin-up offset in the computed system momentum magnitude shown in Figure 3.

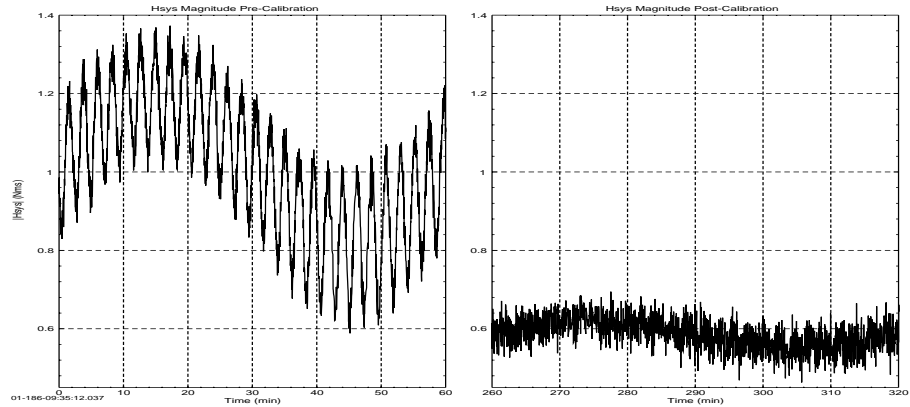


Figure 3: Pre- and Post-Calibration System Angular Momentum Magnitude

Stray light and radiation interference in the phasing loops was less of a problem for the ASTs than anticipated. Both lost track when the Moon was within a degree or so of the FOV, but only for a few seconds in each of at most three spin cycles in any precession cycle; no more than 13 AST readings were lost in any precession cycle. The ASTs have been routinely tracking 15 to 40 stars at L₂, where there is no interference; and attitude knowledge has been better than 20 arcseconds per axis, easily meeting the three-axis root-sum-square requirement of 78 arcseconds. The Sun angle has been maintained between 22.44° and 22.54° in Observing Mode, as shown in Figure 4 by the perfect circle traced by the Sun vector over several hours.

Charged particle flux from extreme solar activity on November 5, 2001 caused a power-on reset of the Mongoose processor. The ACS transitioned autonomously to Safehold Mode in the ACE, which functioned exactly as designed to keep MAP safe. The transition to Safehold Mode was discovered by operations personnel at the next telemetry pass about 12 hours later, and recovery to Observing Mode was accomplished within three hours of this discovery.

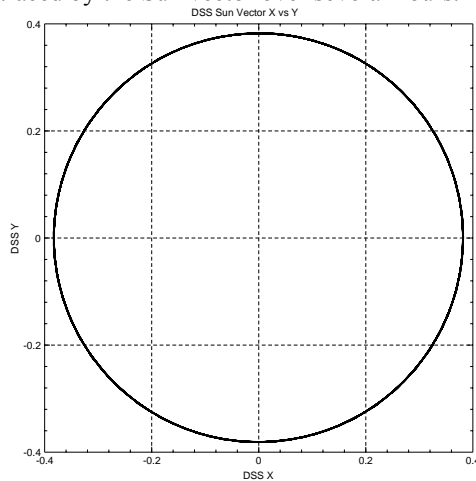


Figure 4: DSS Data in Observing Mode

Conclusions

The attitude control system described in this paper has successfully met the demanding requirements of the Microwave Anisotropy Probe mission. These include the need to function robustly far from the Earth where no magnetic field is useful for sensing or actuation, and with infrequent telemetry passes. The processor upset on November 5, 2001 illustrated the importance of having a safemode control capability that is independent of the primary control hardware and software.

References

1. Boguess, N. W., et al., The COBE Mission: Its Design and Performance Two Years After Launch, *Astrophysical Journal*, vol. 397, no.2, pp. 420-429, 1992
2. Gulkis, S., Lubin, P. M., Meyer, S. S., and Silverberg, R. F., The Cosmic Background Explorer, *Scientific American*, vol.262, no.1, pp.132-139, 1990
3. Smoot, G. F., et al., Structure in the COBE Differential Microwave Radiometer First-Year Maps, *Astrophysical Journal Letters*, vol.396, pp.L1-L5, 1992
4. Bennett, C.L., et al., Four-Year COBE DMR Cosmic Microwave Background Observations: Maps and Basic Results, *Astrophysical Journal Letters*, vol.464, pp.L1-L4, 1996.
5. Bennett, C. L., Hinshaw, G. F., and Page L., A Cosmic Cartographer, *Scientific American*, vol.284, no.1, pp.44-45, 2001 (see also <http://map.gsfc.nasa.gov>)
6. Hu, W., Sugiyama, N., and Silk, J., The Physics of Microwave Background Anisotropies, *Nature*, vol.386, no.6620, pp. 37-43, 1997 (see also <http://background.uchicago.edu>)
7. Richon, K. V., and Mathews, M. W., An Overview of the Microwave Anisotropy Probe (MAP) Trajectory Design, *Astrodynamics 1997, Volume 97, Advances in the Astronautical Sciences*, edited by F. R. Hoots, B. Kaufman, P. J. Cefola, and D. B. Spencer, San Diego, CA, Univelt, Inc. for the American Astronautical Society, pp. 1979-1998, 1998
8. Ericsson-Jackson, A. J., Andrews, S. F., O'Donnell, J. R., Jr., and Markley, F. L., MAP Stability, Design and Analysis, *Spaceflight Dynamics 1998, Volume 100, Advances in the Astronautical Sciences*, edited by Thomas H. Stengle, San Diego, CA, Univelt, Inc. for the American Astronautical Society, pp. 955-969, 1998
9. Wertz, J. R., ed., *Spacecraft Attitude Determination and Control*, Dordrecht, Holland, D. Reidel, 1978
10. Shuster, M. D., A Survey of Attitude Representations, *Journal of the Astronautical Sciences*, vol.41, no.4, pp.439-517, 1993
11. Lefferts, E. J., Markley, F. L., and Shuster, M. D., Kalman Filtering for Spacecraft Attitude Estimation, *Journal of Guidance, Control, and Dynamics*, vol.5, no.5, pp.417-429, 1982
12. Murrell, J. W., Precision Attitude Determination for Multimission Spacecraft, *1978 AIAA Guidance and Control Conference*, AIAA Paper 78-1248, Palo Alto, CA, pp.70-87, 1978
13. Wie, B., and Barba, P. M., Quaternion Feedback for Spacecraft Large Angle Maneuvers, *Journal of Guidance, Control, and Dynamics*, vol.8, no.3, pp.360-365, 1985